J Mater Sci (2011) 46:3162–3168
DOI 10.1007/s10853-010-5199-4

Silver-embedded zeolite crystals as substrates for surface-enhanced Raman scattering

**Ning Liu · Maozhen Gong · Peng Zhang ·
Liangxiong Li · Wenbing Li · Robert Lee**

Received: 14 September 2010 / Accepted: 16 December 2010 / Published online: 29 December 2010

Abstract This paper reports the preparation of a type of Ag-embedded zeolite crystals as surface-enhanced Raman spectroscopy (SERS) substrates by chemical reduction of Ag^+-exchanged ZSM-5. Ag^+ ions were loaded into the zeolite framework by ion exchange. Then the exchanged-Ag^+ ions were reduced and metallic silver clusters formed inside the zeolite channel. The resulting Ag-embedded zeolite crystals are characterized by using a number of techniques including X-ray diffraction, scanning electron microscopy, and X-ray photoelectron spectroscopy to confirm silver formed inside the crystal channel. The fabricated Ag-embedded ZSM-5 zeolite substrates displayed strong and reproducible SERS activity for different Raman probe molecules such as Tris(2,2′-bipyridyl) ruthenium(II) chloride (RuBpy) and rhodamine 6G (R6G). Since silver embedded into the zeolite channel without changing the crystal surface property, the Ag–ZSM-5 zeolite crystal can be used to prepare different SERS-active substrate (SERS-tags), in which different probe molecules may be detected. Such Ag-embedded zeolite substrate would be useful in chemical and biological sensing and in the development of SERS-based analytical devices.

Introduction

Studies on development of practical surface-enhanced Raman spectroscopy (SERS) substrates have drawn broad attention for over 30 years due to the potential applications of SERS in chemical and biological sensing [1–12]. The efficient SERS substrate must not only provide large enhancement factors but also be robust, stable, uniform, and reproducible. It is also desirable that the substrates are easy and relatively inexpensive to fabricate and store. The most commonly used SERS-active substrates are aggregated Ag and Au colloids [13–17]. Ag or Au particles of nanometer sizes have been shown to supply a high Raman enhancement factor. Nie and Emory [18] reported that SERS of single rhodamine 6G molecules was detected when they were absorbed on the silver nanoparticle surface. However, the stability of the colloidal solution and reproducibility of aggregation are two major problems for nano-Ag/Au substrate [19, 20]. Another common substrate is a roughened metal electrode. Although these substrates are more stable than colloids, their enhancement factors are typically not as high. Recently, template-based fabrication methods have been used for SERS substrate preparation and have exhibited promising potentials [21–23]. In particular, nanoporous matrices, such as porous alumina and silica, have been used as templates, and a silver thin film was either coated onto the surface through vacuum deposition or inside the pores by chemical plating. Chan et al. [23] developed a silver-coated nanoporous silicon substrate by depositing a silver thin film inside the nanopores. They observed that such a SERS substrate could exhibit a surface

---

Electronic supplementary material The online version of this article (doi:10.1007/s10853-010-5199-4) contains supplementary material, which is available to authorized users.

N. Liu (✉) · L. Li · R. Lee
Petroleum Recovery Research Center, New Mexico Institute of Mining and Technology, Socorro, NM 87801, USA
e-mail: ningliu@nmt.edu

M. Gong
Department of Petroleum & Natural Gas Engineering, New Mexico Institute of Mining and Technology, Socorro, NM 87801, USA

P. Zhang · W. Li
Department of Chemistry, New Mexico Institute of Mining and Technology, Socorro, NM 87801, USA

enhancement factor of 10^{10}. The advantages of template-based fabrication are that the template can be fabricated over a relatively large area with statistically uniform structures and the required noble metal coating is very thin, rendering the process relatively inexpensive.

In this paper, we report the use of zeolite as SERS-active substrate. Zeolites are crystalline aluminosilicates with unique pore structures, which have been employed in a variety of important industrial processes. Dutta and Robins [24] first reported the use of a silver-coated zeolite as SERS substrates. Silver ions were exchanged into the cages of the Faujasitic (FAU) zeolite, followed by chemical reduction by hydrazine. Silver particles were observed on the surface of the zeolite due to the migration of the exchanged silver ions from the interior of the zeolite to the surface. Yan et al. [25] fabricated zeolite as SERS-active substrate via vacuum deposition of silver on zeolite film. They observed that the prepared substrate could enhance the Raman signal as uranyl ions were adsorbed onto the zeolite surface. In our study, we investigated Na–ZSM-5 zeolite crystal as a potential SERS-active substrate. Ag^+ ions were exchanged inside the zeolite pores and reduced inside. The prepared Ag–ZSM-5 substrate was SERS-active with very good long-term stability.

Experimental

Reagents

Tetrapropylammonium hydroxide (TPAOH), sodium aluminate, RuBpy, and R6G were purchased from Aldrich. Tetraethyl orthosilicate (TEOS, 98%), formaldehyde (37%) was supplied by Acros.

Synthesis of Na–ZSM-5 zeolite crystals

Na–ZSM-5 zeolite crystals were synthesized by the hydrothermal method. The synthesis solution was prepared by mixing 5.65 mL 1 M TPAOH, 10.2 mL TEOS, 0.0739 g $NaAlO_2$, and 30 mL deionized (DI) water. Then the mixture was stirred at 45 °C for 12 h. Hydrothermal treatment was conducted in an autoclave at 180 °C for 4 h. After synthesis, the zeolite crystals were washed, dried, and fired at 500 °C for 6 h to remove the template molecule.

Preparation of Ag–zeolite particles

In order to obtain Ag–zeolite particles, Ag^+-exchanged zeolites were prepared by ion-exchanging the zeolite with 0.1 M $AgNO_3$. 1.0 g calcined Na–ZSM-5 crystals were equilibrated with 100 mL 0.1 M $AgNO_3$ in the dark at room temperature for 24 h. The zeolite powder was next washed with DI water three times to remove the surface-adsorbed Ag^+ ions. Reduction of Ag^+–ZSM-5 crystals was carried out by adding 0.05 g Ag^+–ZSM-5 powders to a solution containing 0.232 mL 0.1 M NaOH, 0.464 mL 0.128 M formaldehyde, and 19.3 mL DI water. The mixture was stirred at room temperature for 12 h. The samples were then extensively washed with DI water to remove any unreacted formaldehyde and dried at 70 °C. The prepared crystals were characterized with field emission scanning electron microscopy (FE-SEM, JEOL 5800LV) operating at 25.0 kV and X-ray diffraction (XRD) with Cu kα radiation. X-ray photoelectron spectroscopy (XPS) was measured with a Kratos AXIS ULTRA X-ray Photoelectron Spectrometer. Inductively coupled plasma mass spectroscopy (ICP-MS) was carried out to determine the composition of the prepared crystals.

SERS measurement

The dye molecules, RuBpy and R6G, were used as the probe molecules to investigate the SERS activity. An 18 mL 0.5 g/L Ag–ZSM-5 solution was first mixed with 2.0 mL 0.1 mM dye solution under vigorous stirring. Next a drop of the solution was cast onto a tilted, clean cover slip and allowed to dry at room temperature. Raman measurements were carried out on a LabRAM Raman microscope. Laser intensities at the samples were set at approximately 130 μW for the 632.8 nm HeNe laser for all measurements. Exposure time for all measurements was 1 s. Each spectrum was the average of 10 scans.

Results

Figure 1 shows the SEM images of Ag^+-exchanged ZSM-5 crystals and energy-dispersive X-ray spectroscopy (EDS) collected on the samples. The SEM images and EDS data clearly indicate that (1) there exist only zeolite crystals and no bulk metal formed at observable size outside the crystals, (2) ion exchange method for preparation of Ag^+–ZSM-5 does not cause any observable defects in the structure of zeolite crystals, (3) silver was successfully loaded in the crystals. Chemical composition of the prepared Ag^+-exchanged ZSM-5 was determined by inductively coupled plasma mass spectroscopy (ICP-MS) (see Table 1S in Supporting Information). 2.3 wt% silver was obtained with an exchange time of 24 h. More silver could be obtained with increasing ion exchange time [26].

Reduction of the exchanged Ag^+ ions was carried out by formaldehyde. Figure 2 shows the SEM image of the reduced Ag–ZSM-5 crystals. Compared with the high magnification SEM image of Ag^+-exchanged ZSM-5 crystals in Fig. 1b, no bulk silver particles were observed

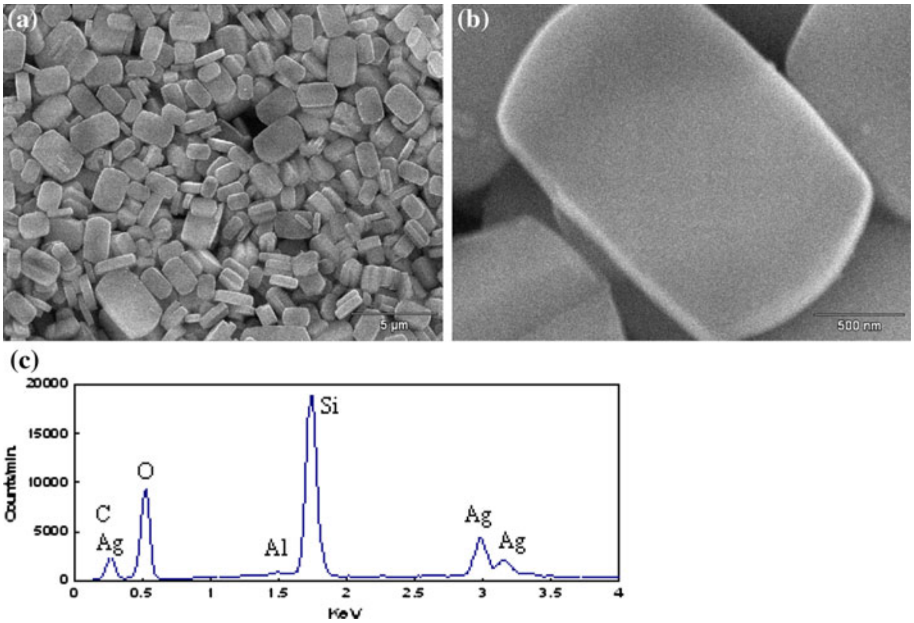

Fig. 1 **a** Low magnification and **b** high magnification SEM images of Ag^+-exchanged ZSM-5 crystals; **c** EDS spectra of the Ag^+-exchanged ZSM-5 crystals

on the Ag–ZSM-5 crystal surface. Figure 2 also revealed that the morphology of the reduced Ag–ZSM-5 crystal was the same as the Ag^+-exchanged ZSM-5, which indicated the reduction reaction did not change or damage the crystal structure. Figure 3 shows the results of the X-ray photoelectron spectroscopy (XPS) spectra of Ag^+–ZSM-5 and Ag–ZSM-5. XPS studies provide the local environment and oxidation state of silver in ZSM-5 crystals. The survey spectrum given in Fig. 3a indicates that silver is the only element detected in addition to the zeolite framework elements, which supports the EDS results in Fig. 1c.

Two probe molecules, RuBpy and R6G, were used to evaluate the SERS activity of the silver-embedded zeolite substrate. Figure 4 compares SERS spectra obtained from Ag–ZSM-5 and Na–ZSM-5 substrates [5, 10]. It can be seen that, under the similar experimental conditions, Ag–ZSM-5 substrate displays very strong SERS of RuBpy, while the Na–ZSM-5 substrate is not SERS-active, indicating that the Raman enhancement is due to the silver component in the Ag–ZSM-5 substrate. Figure 5 displays a series of SERS with different concentrations of RuBpy in Ag–ZSM-5.

To evaluate the SERS enhancement factor for the prepared Ag–ZSM-5 substrate, Na–ZSM-5 zeolite crystals were immersed into 20.0 mL 0.1 M RuBpy, in which the particle concentration of Na–ZSM-5 was the same as that of Ag–ZSM-5, as described above. Then the SERS spectra were taken under the same conditions (laser intensity, integration time). As shown in Fig. 6, the SERS intensity of the RuBpy adsorbed onto the Na–ZSM-5 crystals is obviously lower than that of the Ag–ZSM-5 crystals, even when the RuBpy concentration is 0.1 M for Na–ZSM-5.

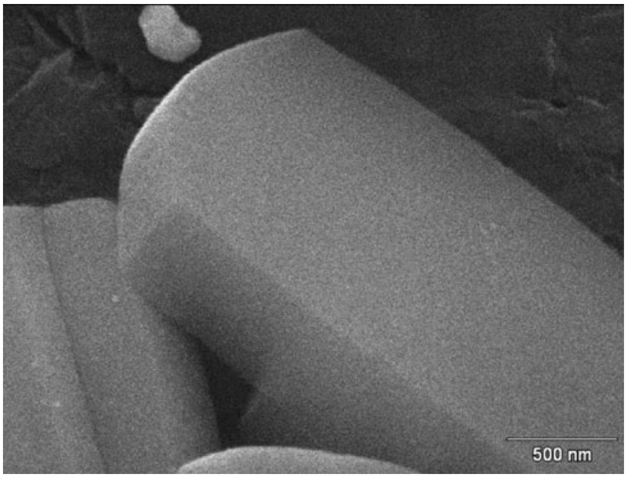

Fig. 2 SEM image of the Ag–ZSM-5 crystals

Discussion

The synthesized Na–ZSM-5 zeolite contains a three-dimensional interconnected five-member ring linked together through oxygen bridges. XRD patterns (see Fig. 1S in Supporting Information) and SEM image (see Fig. 2S in Supporting Information) indicated that the as-synthesized products were well crystallized. The Al^{3+} doped in the synthesis could replace the Si^{4+} in the zeolite framework. To maintain the overall charge neutral, an additional positive charge is required in the zeolite crystal to compensate for the deficient positive charge due to the substitution. The positive charge could be proton or sodium ions, which could then be substituted by other ions such as Ag^+ through ion exchange. After the Ag^+ ions exchanged into

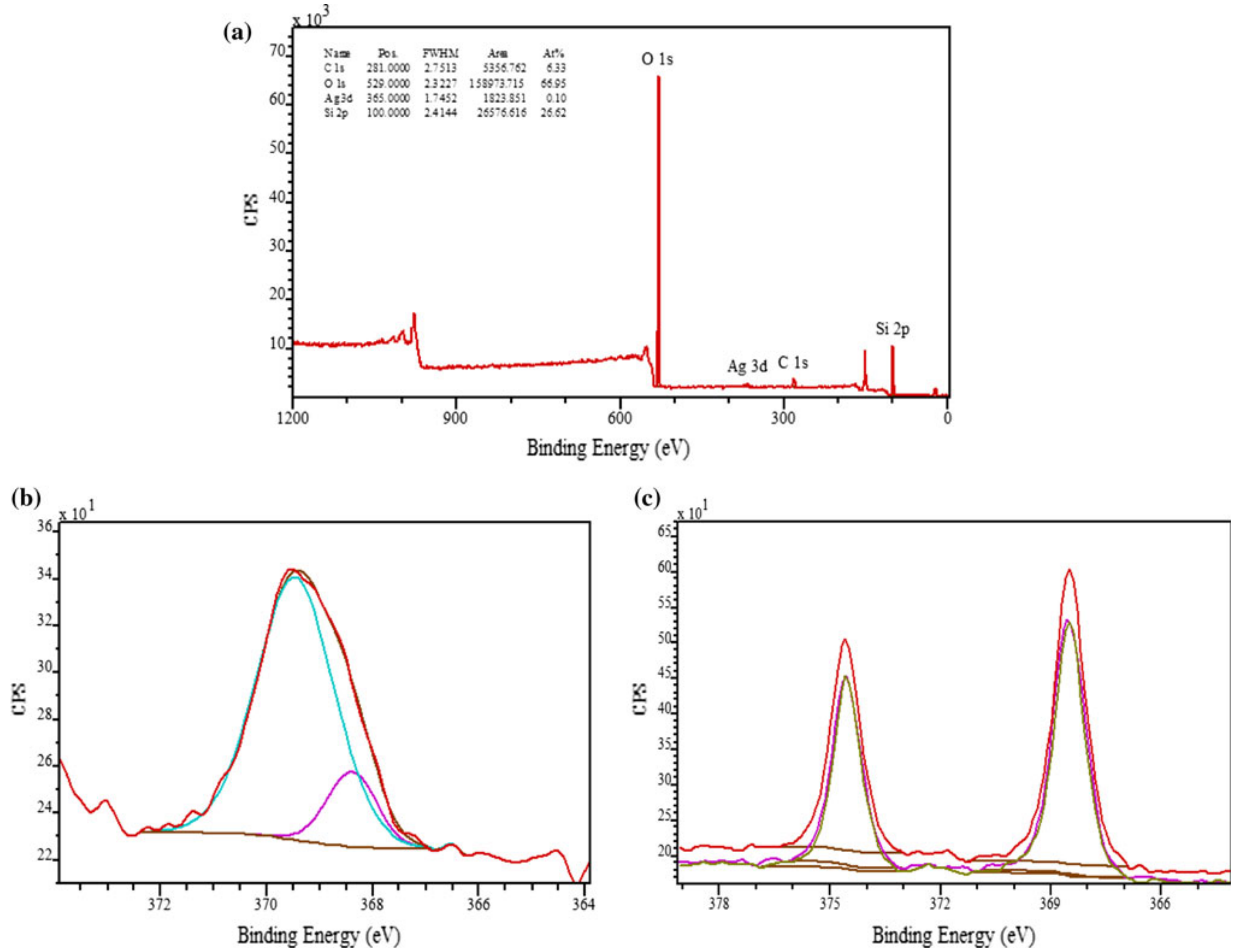

Name	Pos.	FWHM	Area	At%
C 1s	281.0000	2.7513	5356.762	6.33
O 1s	529.0000	2.3227	158973.715	66.95
Ag3d	365.0000	1.7452	1823.851	0.10
Si 2p	100.0000	2.4144	26576.616	26.62

Fig. 3 XPS spectra of Ag^+ and Ag in zeolite crystals. **a** XPS survey scans of Ag^+–ZSM-5, **b** Ag^+ 3*d* XPS spectra, and **c** Ag 3*d* and 2*p* XPS spectra

Fig. 4 SERS spectra of RuBpy and R6G (10^{-5}M)

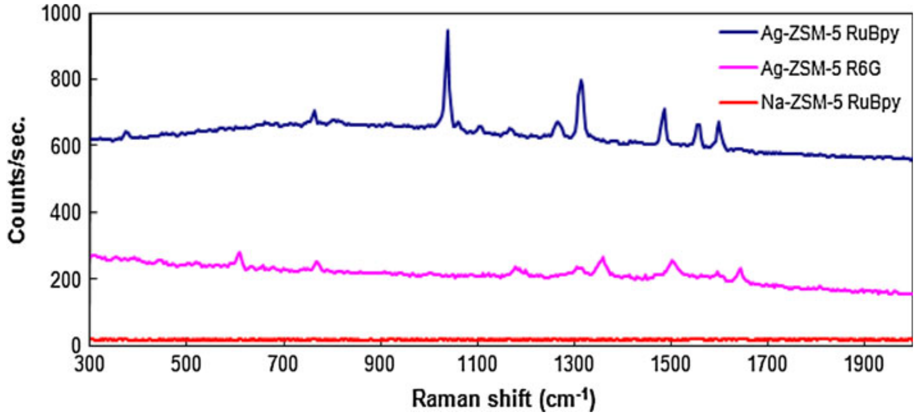

the zeolite channel, they can move or migrate in the channel and form different size of ions clusters. Sazama et al. and Ozin et al. [26, 27] reported ions clusters, such as Ag_3^{2+}, Ag_6^{5+}, and Ag_n^{q+}, formed in the channel of Ag^+-exchanged zeolites and the size of the clusters was in the range of 5.1–7.2 Å.

Various reducing agents, such as formaldehyde, hydrazine, sodium borohydride, and butylamine, can reduce Ag^+

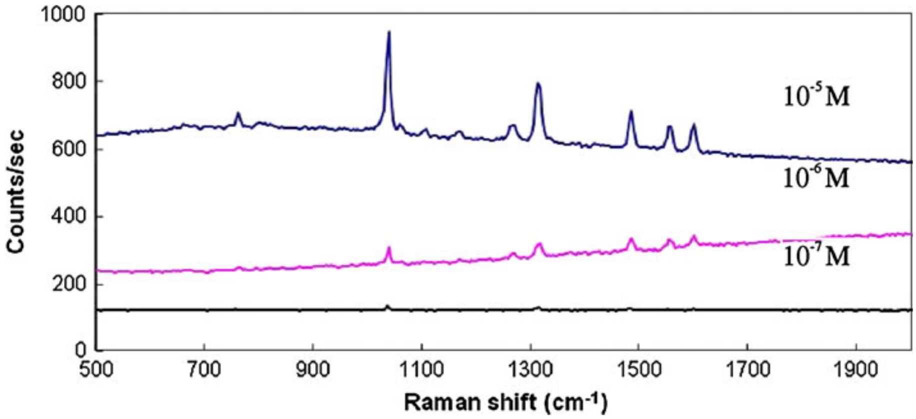

Fig. 5 SERS spectra of RuBpy at different concentration

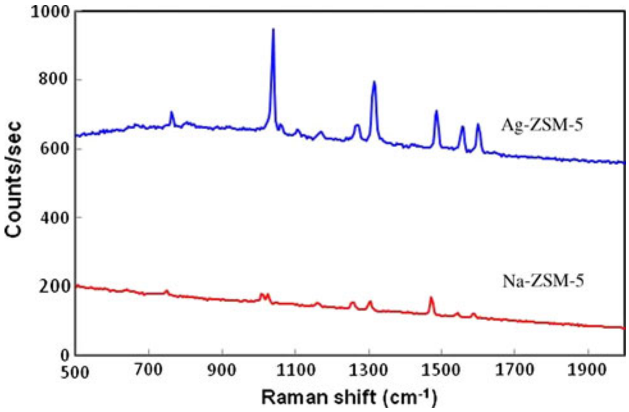

Fig. 6 Raman spectra of RuBpy on Ag–ZSM-5 and Na–ZSM-5 substrates

to Ag. Our choice of formaldehyde was based on the simple reaction and small molecular size. In order to completely reduce all the exchanged Ag^+, NaOH was added to promote the reaction. The added hydroxyl ion undergoes a nucleophilic addition reaction to formaldehyde, producing hydride and formate ions [13]. The hydride ions reduce silver ions to silver atoms with hydrogen as a by-product. The initial ratios of formaldehyde/Ag^+ and OH^-/Ag^+ were 4 and 1, respectively, to completely reduce all exchanged silver ions [13]. The results of XPS spectra in Fig. 3 demonstrated that all the exchanged Ag^+ ions were completely reduced by formaldehyde. It is known that the Ag^+ 3*d* bonding energy peak appears at 368.8 eV, whereas that of metallic silver appears at 368.2 eV. The experimental peak for Ag^+–ZSM-5 was observed at 369.3 eV. The slight difference could be explained by the $Ag_n^{\delta+}$ cluster formed in the zeolite channel [26, 27]. A small peak observed at 368.5 eV was attributed to partial reduction of the silver ions by water in the zeolite channel [27]. After Ag^+ reduction to metallic silver, one peak observed at 368.5 eV was identified as metallic silver 3*d* peak. The other peak, appearing at 374.5 eV, is the silver 2*p* peak due to spin orbital coupling.

We also noticed that most of the exchanged Ag^+ ions were reduced in the zeolite channel because (1) the formaldehyde molecule could easily penetrate into the zeolite channel due to its smaller molecular size; (2) butylamine cannot reduce the exchanged Ag^+ ions but it can reduce the Ag^+ ions in solution [12]. The larger molecular size of butylamine and its spatial configuration rendered it difficult to enter the zeolite channel. No bulk silver metal particles were observed on the Ag–ZSM-5 zeolite surface (Fig. 2). In the pioneering research by Dutta and Robins [24], the exchanged silver ions could migrate from the NaX zeolite interior to the outer surface during reduction. The “snowflake” like patter silver particles with typical dimension of ~2 μm were observed on the zeolite surface. Unlike NaX zeolite, our study of ZSM-5 crystal has smaller pore size and different structure. The difference in pore size and crystal structure between ZSM-5 and NaX may lead to the different mobility of Ag^+ in zeolite pore. In addition, the location of the exchanged Ag^+ ions in zeolite crystals also affects their migration in the crystal [27].

It would be interesting to explore the possible use of the as-synthesized silver-embedded zeolite crystal for fabricating intense SERS substrates to detect different molecules. The probe molecules, RuBpy and R6G, with the molecular size of 13 Å and 10 Å [28, 29], respectively, can be adsorbed onto the zeolite surface. The exchanged silver ions or clusters inside the zeolite pores were reduced, forming silver nanoparticles. These silver nanoparticles were distributed throughout the zeolite crystal. When the probe molecules were adsorbed onto the zeolite crystals, they were brought close to the silver nanoparticles inside the pores, an optical cavity formed. Localized surface plasmons (LSP) can be excited by proper illumination as the cavity is placed into the focus of the laser light. The LSP are associated with electron density oscillations under the influence of the external electromagnetic field, creating in turn their own electromagnetic field [30]. Molecules exposed to this enhanced field lead to enhanced Raman signal. We also noticed that, as the probe molecules were adsorbed onto the zeolite surface, they could not enter the zeolite pore channel due to size exclusion. Therefore, the SERS enhancement observed in these Ag–ZSM-5 crystals is probably due solely to electromagnetic enhancement, as there is no direct contact between the surface-absorbed probe molecules and the reduced silver inside the pores [31]. Li et al. [32] also observed strong SERS as the probe molecules were adsorbed onto the Au/SiO_2 nanoparticles, where there was no direct contact between the probe molecules and the gold core. Since there was no direct contact between the probe molecules and silver particles, any molecules attracted by the zeolite crystal could be detected. Hence, the Ag–ZSM-5 can be used as SERS substrate for the in situ detection of various molecules.

The as-synthesized Ag–ZSM-5 substrate can detect RuBpy concentrations as low as 10^{-7} M in solution (Fig. 5). The detection limit could be further improved by increasing the ion exchange time, which would result in more Ag^+ ions being exchanged in the zeolite pores and more SERS-active silver nanoparticles spread throughout the zeolite crystal. Furthermore, due to the chemical and physical stability of the zeolite crystals, no aggregation of silver nanoparticles was observed for the prepared substrate after long-term storage. The as-synthesized Ag–ZSM-5 substrate displayed similar SERS activity after 1 month.

The SERS enhanced factor (EF) for Ag–ZSM-5 crystals was estimated using the following relationship:

$$\mathrm{EF} = (I_{\mathrm{SERS}}/I_{\mathrm{NR}})(N_{\mathrm{NR}}/N_{\mathrm{SERS}})$$

where I_{SERS} and I_{NR} are the Raman scattering intensity of RuBpy on Ag–ZSM-5 and Na–ZSM-5 crystals, respectively, and N_{SERS} and N_{NR} are the numbers of RuBpy molecules illuminated by the laser light to obtain the corresponding Raman spectra. I_{SERS} and I_{NR} were measured at different wavelengths, and the ratio of N_{NR} and N_{SERS} was estimated with the RuBpy concentrations since the particle size and concentration in both solutions were the same. The ratios of I_{SERS} and I_{NR} at 1031 cm^{-1}, 1317 cm^{-1}, 1485 cm^{-1}, 1556 cm^{-1}, and 1600 cm^{-1} were measured (shown in Fig. 6); these were 13.8, 6.1, 2.2, 7.3, and 8.4, respectively. The EF for Ag–ZSM-5 was estimated in the range of 2.2×10^4–1.38×10^5. The value is quite comparable to that observable from the usual nanostructured silver substrates [33, 34].

Conclusions

In summary, a very stable SERS-active Ag–ZSM-5 substrate was fabricated. Ag^+ ions were first loaded into the zeolite channel through ion exchange and then reduced inside the zeolite pores by formaldehyde. The method is cost-effective and easy to synthesize. The characterization by means of SEM, EDS, and XPS indicated that the formation of silver nanoparticles in the zeolite channel. The prepared Ag–ZSM-5 substrate displayed strong SERS activity and was stable for a long period of time. The formation of silver nanoparticles inside the zeolite pores may behave as a “hot spot” to enhance the Raman signals of molecules adsorbed on the zeolite surface. The advantages of the zeolite substrate for SERS include ease of preparation, very good stability, and reproducibility, as well as the possibility of using SERS to detect various molecules in situ. We believe that these Ag–ZSM-5 SERS substrates will be useful in the development of SERS-based analytical devices.

Acknowledgements Support for this research came from the Water Innovation Fund of the State of New Mexico and Natural Science Foundation (CHE-0632071). The authors would like to thank Ms. Liz Bustamante for the assistance in preparing the manuscript.

References

1. Jeanmaire D, Van Duyne R (1977) J Electroanal Chem 84:1
2. Fernández-López C, Mateo-Mateo C, Álvarez-Puebla R, Pérez-Juste J, Pastoriza-Santos I, Liz-Marzán L (2009) Langmuir 25:13894
3. Wang W, Gu B (2005) Appl Spectrosc 59:1509
4. Wang Y, Ruan W, Zhang J, Yang B, Xu W, Zhao B, Lombardi J (2009) J Raman Spectrosc 40:1072
5. Lin Z, Chang H (2008) Langmuir 24:365
6. Ruan C, Eres G, Wang W, Zhang Z, Gu B (2007) Langmuir 23:5757
7. Geissler M, Li K, Cui B, Clime L, Veres T (2009) J Phys Chem C 113:17296
8. Shi C, Yan H, Gu C, Ghosh D, Seballos L, Chen S, Zhang J, Chen B (2008) Appl Phys Lett 92:103107
9. Zhao Y, Newton J, Liu J, Wei A (2009) Langmuir 25:13833
10. Zhang P, Guo Y (2009) J Am Chem Soc 131:3808
11. Bao F, Yao J, Gu R (2009) Langmuir 25:10782
12. Kim K, Lee H, Park H, Shin K (2008) J Colloid Interface Sci 318:195
13. Chou K, Ren C (2000) Mater Chem Phys 64:241
14. Huang Y, Yang Y, Chen Z, Li X, Nogami M (2008) J Mater Sci 43:5390. doi:10.1007/s10853-008-2793-9
15. Fan JG, Zhao YP (2008) Langmuir 24:14172
16. Rivas L, Sanchez-Cortes S, Carcía-Ramos JV, Morcillo G (2001) Langmuir 17:574
17. Nickel U, Castell A, Pöppl K, Schneider S (2000) Langmuir 16:9087
18. Nie S, Emory S (1997) Science 275:1102
19. Michaels AM, Jiang J, Brus L (2000) J Phys Chem B 104:11965
20. Chen SP, Hosten CM, Vivoni A, Birke RL, Lombardi JR (2002) Langmuir 18:9888
21. Chen Y, Kim H (2007) Mater Lett 61:5040
22. Lin H, Mock J, Smith D, Gao T, Sailor M (2004) J Phys Chem B 108:11654
23. Chan S, Kwon S, Koo T, Lee L, Berlin A (2003) Adv Mater 15:1595
24. Dutta PK, Robins D (1991) Langmuir 7:2004
25. Yan W, Bao L, Mahurin S, Dai S (2004) Appl Spectrosc 58:18

26. Sazama P, Jirglová H, Dědeček J (2008) Mater Lett 62:4239
27. Ozin G, Hugues F, Mattar S, McIntosh D (1983) J Phys Chem 87:3445
28. Ruda-Eberenz T, Nagy A, Waldman W, Dutta P (2008) Langmuir 24:9140
29. Avnir D, Levy D, Reisfeld R (1984) J Phys Chem 88:5956
30. Pettinger B, Ren B, Picardi G, Schuster R, Ertl G (2004) Phys Rev Lett 92:096101
31. Schatz GC, Van Duyne RP (2002) In: Chalmers JM, Griffiths PR (eds) Handbook of vibrational spectroscopy. Wiley & Sons, Chichester, UK
32. Li J, Huang Y, Ding Y, Yang Z, Li S, Zhou X, Fan F, Zhang W, Zhou Z, Wu D, Ren B, Wang Z, Tian Z (2010) Nature 464:392
33. Park H, Yoon J, Kim K (2006) Langmuir 22:1626
34. Li D, Li DW, Li Y, Fossey J, Long Y (2010) J Mater Chem 20:3688